Postbuckling Analysis of Functionally Graded Beams Using Nonlinear Model

Khaled Amara[1*], Mokhtar Bouazza[2], Bourada Fouad[1]

Abstract

The major novelty of the paper in the study, post-buckling of simply supported FGM beams using various theory, classical beam theory (CBT), first-order shear deformation beam theory (FSDBT), parabolic shear deformation beam theory (PSDBT) and exponential shear deformation beam theory (ESDBT). Governing equations of FGM beam for post-buckling problem were found by applying Hamilton principle and Navier type solution method was used to solve post-buckling problem. It is assumed that elasticity modulus is changing in the thickness direction and all other material properties are taken to be constant. Variation of elasticity modulus in the thickness direction, are described by a simple power law distribution in terms of the volume fractions of constituents. The shear effect is shown to have a significant contribution to both the buckling and post-buckling behaviors. Results of this analysis show that classical and first-order theories underestimate the amplitude of buckling while all higher order theories, considered in this study, yield very close results for the static post-buckling response.

Keywords

Buckling, Amplitude, Shear deformation, Functionally graded beams

[1] Department of Civil Engineering, University Center of Ain Temouchent, 46000, Algeria

[2] Department of Civil Engineering, University of Bechar, 8000, Algeria

[*] Corresponding author, e-mail: kamara2003dz@yahoo.fr

1 Introduction

Functionally graded materials (FGMs) are novel, microscopically inhomogenous in which the mechanical properties vary smoothly and continuously from one surface to another. It has many favorable performances in engineering applications, such as high resistance to large temperature gradients, reduction of stress concentration and so on. Therefore, FGMs have been applied extensively in many situations where large temperature gradients are encountered. And the studies of the mechanical behaviors of FGM structures under the thermal and mechanical loads have being attracted more and more attentions and also have become a new research field in solid mechanics.

A brief overview of recent works about thermo-mechanical analysis of functionally graded structures is presented below. Several applications of the theory of thermo-elasticity can be found in the book by Hetnarski and Eslami [1]. In particular, the thermal stress analysis of beams based on Euler–Bernoulli assumptions was presented. Beams made of functionally graded materials were also investigated. The problem of thermal stresses in FGMs was addressed by Noda [2]. The optimal gradation profiles to decrease the thermal stresses in FGMs were discussed. The thermoelastic behaviour of functionally graded beams was also studied by Chakraborty et al. [3]. A beam finite element based on Timoshenko's theory was developed, accounting for an exponential and a power law through-the-thickness variation of elastic and thermal properties. Zhao et al. [4] studied the post-buckling of simply supported rod made of functionally graded materials under uniform thermal loading using the numerical shooting method. Li et al. [5] studied the thermal post-buckling behaviour of a fixed-fixed beam based on the Timoshenko beam theory. They found the effect of shear on buckling of homogeneous beams and used the shooting method to analyze the post-buckling behaviour of FGM beams. Rastgo et al. [6] discussed the buckling of functionally graded material curved beams under linear thermal loading. They studied both the in-plane and out of plane buckling of curved beams. Ke et al. [7] presented the post-buckling of a cracked beam for hinged–hinged and clamped–hinged edge conditions based on the Timoshenko beam theory. Also, Ke et al. [8] presented the

free vibration and mechanical buckling of cracked beams using the first order shear deformation beam theory for three types of boundary conditions.

Recently, considerable interest has also been focused on investigating the performance of FGM plates. For example, Reddy [9] proposed an analytical formulation relied on a Navier's approach using the third-order shear deformation theory and the von Karman-type geometric non-linearity. Veland Batra [10, 11] introduced an exact formulation based on a power series for thermoelastic deformations and vibration of rectangular FGM plates. Matsunaga [12, 13] used a two-dimensional global higher-order deformation theory to analyze free vibration and buckling of FGM plates. In thermal buckling of functionally graded material plates Bouazza et al. [14, 15] discussed the thermal buckling of plates based on the classical and first order displacement plate theories. They studied three types of thermal loadings for critical bucking temperature of plates and found that the classical plate theory over-predicts the buckling behaviour of thick plates. Also, Bouazza et al. [16, 17] expressed the mechanical buckling of plates under three types of mechanical loadings for simply supported plates in all edges. Effects of changing plate characteristics, material composition, and volume fraction of constituent materials on the critical temperature difference of FGM with simply supported edges are also investigated. They observed in their study that transverse shear deformation has considerable effects on the critical buckling temperature of FGM plate, especially for a thick plate or a plate with large aspect ratio. The static response of functionally graded plates subjected to thermal loads was addressed by Brischetto et al. [18]. The temperature field was determined by solving Fourier's equation. Different volume fractions of the material constituents were considered to evaluate the temperature, displacement and stress distributions. Hosseini-Hashemi et al. [19], have recently proposed a novel exact analytical approach to free vibration analysis of Levy-type FGM rectangular plates, etc. Due to the complexity of mathematics, it is in general difficult to obtain the exact solution for all problems. Therefore, numerical methods have been devised to solve such FGMs structural components. Nowadays, the finite element method has become the most powerful and reliable tool to analyze FGM structures [20].

In this study, the nonlinear response of simply supported FGM beams is presented. The material properties of the beams vary continuously in the thickness direction according to the power-law form. The formulations are developed by using CBT, FSDBT, PSDBT, and ESDBT. Governing equations were found by applying Hamilton's principle. Navier type solution method was used to obtain critical buckling loads. Different higher order shear deformation theories, first-order shear deformation beam theory and classical beam theories were used in the analysis. In this study, the effects of slenderness ratio, material variations, the different formulations and the beam theories on the first critical buckling load are examined.

2 Presentation of the study area
2.1 Material properties

Consider a rectangular beam made of a mixture of metal and ceramic as shown in Fig. 1. The material in top surface and in bottom surface is metal and ceramic respectively. The modulus of elasticity E, and the Poisson's ratio m are assumed as [21]:

$$E(z) = E_c V_c + E_m (1 - V_c)$$
$$v(z) = v_0 \tag{1}$$

Where E_c and E_m denote values of the elasticity modulus at the top and bottom of the beam, respectively, and V_c denotes the volume fraction of the ceramic and is assumed as a power function as follows:

$$V_c = \left(\frac{z}{h} + \frac{1}{2} \right)^k \tag{2}$$

Where k is a variable parameter. According to this distribution, bottom surface ($z = -h/2$) of functionally graded beam is pure metal, whereas the top surface ($z = h/2$) is pure ceramics, and for different values of k one can obtain different volume fractions of ceramic.

Where z is the thickness coordinate variable; and $-h/2 \leq z \leq h/2$ where h is the thickness of the beam and k is the power law index that takes values greater than or equals to zero.
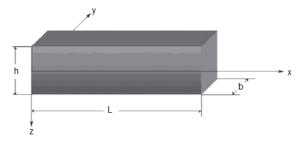

Fig. 1 Co-ordinates and geometry of functionally graded beam.

Figure 2 shows the variation of volume fractions of ceramic in the thickness direction of FGM beam. Here, volume fraction for ceramic increases from 0 at $z = -h/2$ to 1 at $z = h/2$.

The state of stress in the beam is given by the generalized Hooke's law as follows:

$$\sigma_x = Q_{11} \varepsilon_x \ , \ \tau_{xz} = Q_{55} \gamma_{xz} \tag{3}$$

Where Q_{ij} are the transformed stiffness constants in the beam co-ordinate system and are defined as:

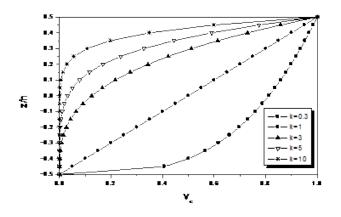$$Q_{11} = E(z), \quad Q_{55} = \frac{E(z)}{2(1+v)} \tag{4}$$

Fig. 2 Volume fraction of ceramic along the thickness direction

2.2 Governing equations

Assuming that the deformations of the beam are in the x–z plane and denoting the displacement components along the x, y and z directions by U, V and W, respectively, the following displacement field for the beam is assumed on the basis of the general shear deformable shell theory presented by Soldatos and Timarci [22]:

$$U(x,z,t) = u(x,t) - zw'(x,t) + f(z)u_1(x,t)$$
$$V(x,z,t) = 0 \qquad\qquad (5)$$
$$W(x,z,t) = w(x,t)$$

Here, u and w represent middle surface displacement components along the x and z directions, respectively, while u_1 is an unknown function that represents the effect of transverse shear strain on the beam middle surface, and $f(z)$ represents the shape function determining the distribution of the transverse shear strain and stress through the thickness.

Classical beam theory is obtained as a particular case by taking the shape function as zero. Although different shape functions are applicable, only the ones which convert the present theory to the corresponding parabolic shear deformation beam theory (PSDBT), first order shear deformation beam theory (FSDBT) and exponential shear deformation beam theory (ESDBT) are employed in the present study. This is achieved by choosing the shape functions as follows:

$$\text{CBT}: f(z) = 0$$
$$\text{FSDBT}: f(z) = z$$
$$\text{PSDBT}: f(z) = z\left(1 - 4z^2/3h^2\right) \qquad (6)$$
$$\text{ESDBT}: f(z) = z\exp\left[-2\left(z/h\right)^2\right]$$

According to the small-strain, moderate-rotation approximations, the nonvanishing strains are given as follows:

$$\varepsilon_x = \frac{\partial U}{\partial x} + \frac{1}{2}\left(\frac{\partial W}{\partial x}\right)^2$$
$$\gamma_{xz} = \frac{\partial U}{\partial z} + \frac{\partial W}{\partial x} \qquad (7)$$

Where ε_x is the normal strain and γ_{xz} is the engineering shear strain.

Here the axial displacement u is assumed to be of order w^2, which is based on the insignificant effect of the inplane inertia, see Nayfeh and Mook [23]. Substituting Eq. (5) into Eq. (7) yields

$$\varepsilon_x = u' + \frac{1}{2}w'^2 - zw'' + fu_1'$$
$$\gamma_{xz} = f'u_1 \qquad\qquad (8)$$

The following stress resultants are introduced [24, 25]:

$$N = \int_A \sigma_x dA, \quad M = \int_A z\sigma_x dA, \quad M^s = \int_A f\sigma_x dA,$$
$$Q^s = \int_A f'\tau_{xw}dA, \qquad (9)$$

Where N and M are the classical well-known force and moment stress resultants, Q^s and M^s are stress resultants associated with the shear deformation. Using Hook's law, the stress resultants are expressed in terms of the strains as follows:

$$\begin{Bmatrix} N \\ M \\ M^S \end{Bmatrix} = \begin{bmatrix} A_{11} & B_{11} & E_{11} \\ B_{11} & D_{11} & F_{11} \\ E_{11} & F_{11} & H_{11} \end{bmatrix} \begin{Bmatrix} u' + \frac{1}{2}w'^2 \\ -w'' \\ u_1' \end{Bmatrix}, \qquad (10a)$$

$$Q^s = A_{55}u_1 \qquad (10b)$$

The extensional, coupling and bending rigidities appearing in Eq. (10a) are, respectively, defined as follows:

$$\left(A_{11}, B_{11}, D_{11}, E_{11}, F_{11}, H_{11}\right) = \int_A \left(1, z, z^2, f(z), zf(z), f(z)^2\right) Q_{11} dA, \qquad (11)$$

Moreover, the transverse shear rigidity appearing in Eq. (10b) is defined according to

$$A_{55} = \int_A K_s f'^2 \overline{Q}_{55} dA \qquad (12)$$

Where Ks is the shear-correction factor for Timoshenko theory ($K_s = 5/6$) that is equal to unity for higher-order shear deformation.

It should be pointed out that the extensional A_{11}, coupling B_{11} and bending D_{11} rigidities are the ones usually appearing even in the classical beam theories. Among the additional rigidities in Eq. (10a), the one denoted as E_{11} is considered as additional coupling rigidity while the ones denoted as F_{11} and H_{11} are considered as additional bending rigidities.

The total potential energy can be expressed as follows:

$$V = \frac{1}{2}\int_v \left(\sigma_x \varepsilon_x + \tau_{xz}\gamma_{xz}\right)dv + \frac{1}{2}\overline{N}\int_0^L w'^2 dx \qquad (13)$$

Substituting Eq. (8) into Eq. (13) and noting the definition of the stress resultants, the potential energy can be expressed as follows:

$$V = \frac{1}{2}\int_0^L \left[N\left(u' + \frac{1}{2}w'^2 \right) - Mw'' + M^s u_1' + Q^s u_1 + \overline{N}w'^2 \right] dx \quad (14)$$

The kinetic energy of the FGM beam is given by

$$T = \frac{1}{2}\int_v \rho \left(\dot{U}^2 + \dot{w}^2 \right) dv = \frac{1}{2}\int_v \rho \left[\left(\dot{u} - z\dot{w}' + f\dot{u}_1 \right)^2 + \dot{w}^2 \right] dv \quad (15)$$

Where ρ is the mass density per unit volume.

Hamilton's variational principle states that at two specified times t1 and t2 is a stationary point (a point where the variation is zero), of the action functional

$$\int_{z_1}^{z_2} \left(\delta T - \delta V + \delta W_{nc} \right) dt = 0 \quad (16)$$

Where δ is the first variation and W_{nc} is the work done by nonconservative forces, δV the virtual total potential energy and δT the virtual kinetic energy of the FGM beam. Applying this principle yields the following equations of motion:

$$-m_0\ddot{u} - m_{01}\ddot{u}_1 - c_u\dot{u} + m_1\ddot{w}' + N' + F_u = 0 \quad (17)$$

$$-m_0\ddot{w} - m_1\ddot{u}'' - m_{11}\ddot{u}_1' + m_2\ddot{w}'' - c_w\dot{w} + M'' + \left(Nw' \right)'$$
$$-\overline{N}w'' + F_w = 0 \quad (18)$$

$$-m_{01}\ddot{u} - m_{02}\ddot{u}_1 + m_{11}\ddot{w}' + M'^s - Q^s = 0 \quad (19)$$

Where

$$m_0 = \rho(z), m_1 = \rho(z)z, m_2 = \rho(z)z^2, m_{01} = \rho(z)f(z),$$
$$m_{02} = \rho(z)f^2(z), m_{11} = z\rho(z)f(z) \quad (20)$$

The equations of motion can be expressed in terms of the displacements, u, w and u_1. To this end, we substitute Eqs. (10a) and (10b) into Eqs. (17)–(19) and obtain

$$-m_0\ddot{u} - m_{01}\ddot{u}_1 + m_1\ddot{w}' - c_u\dot{u} + A_{11}\left(u' + \frac{1}{2}w'^2 \right)'$$
$$+E_{11}u_1'' - B_{11}w''' + F_u = 0 \quad (21)$$

$$-m_0\ddot{w} - m_1\ddot{u}'' - m_{11}\ddot{u}_1' + m_2\ddot{w}'' - c_w\dot{w} + A_{11}\left(w'u' + \frac{1}{2}w'^3 \right)'$$
$$+E_{11}\left(w'u_1' \right)' + B_{11}u''' + F_{11}u_1''' - D_{11}w''' - \overline{N}w'' + F_w = 0 \quad (22)$$

$$-m_{01}\ddot{u} - m_{02}\ddot{u}_1 + m_{11}\ddot{w}' + E_{11}\left(u' + \frac{1}{2}w'^2 \right)'$$
$$+H_{11}u_1'' - F_{11}w''' - A_{55}u_1 = 0 \quad (23)$$

The boundary-value problem governing the static postbuckling response, expressed in terms of stress resultants, can be obtained from Eqs. (17)–(19) by setting all time-dependent terms equal to zero and disregarding the nonconservative forces. The result is:

$$\frac{dN}{dx} = 0 \quad (24)$$

$$\frac{dM^2}{dx^2} + \frac{d}{dx}\left(N\frac{dw}{dx} \right) - \overline{N}\frac{d^2w}{dx^2} = 0 \quad (25)$$

$$\frac{dM^s}{dx} - Q^s = 0 \quad (26)$$

As it is evident from Eq. (24), the stress resultant N, which is the total axial force exerted on the beam's cross section, is a constant. In the context of linear analysis, where the contribution of the midplane stretching is negligible, the induced axial force is simply equal to the externally applied axial load at the beam ends. As a matter of fact, the midplane stretching introduces a tension force on the beam's cross section. As a result, the total axial force N, which is a constant according to Eq. (24), will account for the applied axial force and the induced axial force due to midplane stretching. This means that for a compressive external axial force N, the stress resultant N will be less than the applied force by an amount that is equal to tension due to midplane stretching. Consequently, Eq. (25) that governs the transverse displacement w will be nonlinear. To this end, we express the equations governing the static response of the beam in terms of the displacements. Equations (24)–(26) can be expressed as follows:

$$A_{11}\left(u' + \frac{1}{2}w'^2 \right)' - B_{11}w''' + E_{11}u_1'' = 0 \quad (27)$$

$$A_{11}\left[\left(u' + \frac{1}{2}w'^2 \right)w' \right]' + E_{11}\left(w'u_1' \right)' + B_{11}u'''$$
$$+F_{11}u_1''' - D_{11}w''' - \overline{N}w'' = 0 \quad (28)$$

$$E_{11}\left(u' + \frac{1}{2}w'^2 \right)' - F_{11}w''' + H_{11}u_1'' - A_{55}u_1 = 0 \quad (29)$$

One notes that Eq. (27) may be solved for the axial displacement u, and hence it can be eliminated from the other two equations. This will lead to a flexural model that is given in terms of only the displacements unknowns w and u_1. It is worth noting that this is applicable regardless of the symmetry property of the structural laminate. Integrating Eq. (27) with respect to the spatial coordinate x yields

$$A_{11}\left(u' + \frac{1}{2}w'^2 \right) - B_{11}w'' + E_{11}u_1' = c_1 \quad (30)$$

Where c_1 is a constant that represents the induced axial tension force due to midplane stretching as it will be shown. Integrating Eq. (30) once more, we obtain

$$u(x) = -\frac{1}{2}\int_0^x w'^2 d\xi + \frac{B_{11}}{A_{11}}w' - \frac{E_{11}}{A_{11}}u_1 + \frac{c_1}{A_{11}}x + c_2 \quad (31)$$

For the midplane stretching to be significant, the beam ends must be restrained [26]. The boundary conditions for the axial displacement are assumed as follows:

u = 0 at x = 0; L

The constants c_1 and c_2 are now given by

$$c_2 = \frac{1}{A_{11}}\left[E_{11}u_1(0) - B_{11}w'(0)\right]$$

$$c_1 = \frac{A_{11}}{2L}\int_0^L w'^2 dx + \frac{E_{11}}{L}\left[u_1(L) - u_1(0)\right] - \frac{B_{11}}{L}\left[w'(L) - w'(0)\right]$$

$$(32)$$

Now, Eq. (30) can be rewritten as follows:

$$u' + \frac{1}{2}w'^2 = \frac{1}{2L}\int_0^L w'^2 dx - \frac{E_{11}}{A_{11}}u_1' + \frac{B_{11}}{A_{11}}w' + \frac{E_{11}}{LA_{11}}\left[u_1(L) - u_1(0)\right]$$

$$-\frac{B_{11}}{LA_{11}}\left[w'(L) - w'(0)\right]$$

$$(33)$$

Equation (27) and its first derivative can be expressed as follows:

$$\left(u' + \frac{1}{2}w'^2\right)' = -\frac{E_{11}}{A_{11}}u_1'' + \frac{B_{11}}{A_{11}}w''' \quad (34)$$

and

$$u''' = -\left(w'w''\right)' - \frac{E_{11}}{A_{11}}u_1''' + \frac{B_{11}}{A_{11}}w'''' \quad (35)$$

Substituting Eqs. (33)–(35) into Eqs. (28) and (29), we obtain

$$\left(\frac{B_{11}^2}{A_{11}} - D_{11}\right)w''' - \left(\overline{N} - \frac{A_{11}}{2L}\int_0^L w'^2 dx\right)w''$$

$$+\left(F_{11} - \frac{B_{11}E_{11}}{A_{11}}\right)u_1'' + \beta w'' = 0$$

$$(36)$$

$$\left(H_{11} - \frac{E_{11}^2}{A_{11}}\right)u_1'' + \left(\frac{B_{11}E_{11}}{A_{11}} - F_{11}\right)w''' - A_{55}u_1 = 0 \quad (37)$$

Where β is a constant defined by

$$\beta = \frac{1}{L}\left\{E_{11}\left[u_1(L) - u_1(0)\right] - B_{11}\left[w'(L) - w'(0)\right]\right\} \quad (38)$$

In view of Eqs. (10a) and (10b), the stress resultants M and M^s are given by

$$M = -D_{11}w'' + F_{11}u_1'$$
$$M^s = -F_{11}w'' + H_{11}u_1'$$
$$(39)$$

These two equations can be solved for w^s and u_1' at the boundaries and obtain

$$\left(F_{11}^2 - H_{11}D_{11}\right)w''(\xi) = 0 \quad (40)$$

$$\left(F_{11}^2 - H_{11}D_{11}\right)u_1'(\xi) = 0, \quad (41)$$

With $\xi = 0, L$

Since F_{11}, H_{11}, and D_{11} do not vanish, the boundary conditions in terms of the displacements can be expressed as follows:

$$w = 0 \quad \text{and} \quad u_1' = 0 \quad \text{at} \quad x = 0, L \quad (42)$$

The first buckling mode was proofed to be the only stable equilibrium position. For simply supported boundary conditions outlined above, the following displacement field is assumed:

$$w(x) = a\sin\pi\frac{x}{L} \quad (43)$$

$$u_1(x) = b\cos\pi\frac{x}{L} \quad (44)$$

Where a and b are unknowns to be determined. Substituting Eqs. (43) and (44) into Eqs. (36) and (37), yields three solutions: the first is the trivial solution, $a = 0$, that corresponds to the equilibrium position in the prebuckling state and the other two solutions, $a \neq 0$, correspond to the stable equilibrium positions in the postbuckling state. As it is well-known, the prebuckling equilibrium position becomes unstable beyond the state of buckling. The postbuckling response can be obtained as follows:

$$a = \pm\frac{2}{\pi\sqrt{A_{11}}}\sqrt{\overline{N}L^2 - \pi^2 D_{11} + \frac{\pi^4 F_{11}^2}{L^2 A_{55} + \pi^2 H_{11}}} \quad (45)$$

We note that the buckling amplitude a corresponds to the maximum buckling level that occurs at the midspan of the beam where $x = L/2$.

On the other hand, the critical buckling load, $\overline{N}_{cr}$, can be obtained by solving the linear counterpart of Eq. (36). The result is

$$\overline{N}_{cr} = \frac{\pi^2}{L^2}\left(D_{11} - \frac{\pi^2 F_{11}^2}{L^2 A_{55} + \pi^2 H_{11}}\right) \quad (46)$$

3 Results and discussion

The constituent material properties of the FGM beam were chosen as follows [14-19]:

Al: $E_m = 70 GPa$; $v_c = 0.3$;
Ceramic: $E_c = 380 GPa$; $v_c = 0.3$.

The nondimensional critical buckling load, $\overline{P}_{cr}$, is defined as follows:

$$\overline{P}_{cr} = \frac{L^2}{bh^3 E_m} \overline{N}_{cr} \qquad (47)$$

Non-dimensional first critical buckling load were given in Tables 1-5 for L/h = 5, 10, 20, 50 and 100, respectively, for different theories and for different material distributions. It is seen from the tables that critical buckling load is decreasing with increasing k and increasing with increasing L/h ratios. Difference between the critical buckling load predicted by CBT and shear deformation theories is decreasing with increasing L/h ratio.

Table 1 Comparison of nondimensional first critical buckling load with different theories for different material distribution (L/h = 5, a = 0).

Theory	Ceramic	k = 0.3	k = 1	k = 3	k = 5	k = 10	Metal
CBT	4.906	3.812	2.905	2.305	2.047	1.688	0.904
FSDBT	4.485	3.498	2.655	2.069	1.824	1.4999	0.826
PSDBT	4.4097	3.447	2.611	1.996	1.741	1.433	0.812
ESDBT	4.413	3.721	2.613	1.995	1.737	1.433	0.813

Table 2 Comparison of nondimensional first critical buckling load with different theories for different material distribution (L/h = 10, a = 0).

Theory	Ceramic	k = 0.3	k = 1	k = 3	k = 5	k = 10	Metal
CBT	4.906	3.812	2.905	2.305	2.047	1.688	0.904
FSDBT	4.794	3.728	2.838	2.241	1.987	1.636	0.883
PSDBT	4.772	3.714	2.825	2.219	1.961	1.616	0.879
ESDBT	4.773	3.788	2.826	2.219	1.9598	1.616	0.879

Table 3 Comparison of nondimensional first critical buckling load with different theories for different material distribution (L/h = 20, a = 0).

Theory	Ceramic	k = 0.3	k = 1	k = 3	k = 5	k = 10	Metal
CBT	4.906	3.812	2.905	2.305	2.047	1.688	0.904
FSDBT	4.878	3.791	2.888	2.288	2.032	1.674	0.899
PSDBT	4.872	3.787	2.885	2.283	2.025	1.669	0.897
ESDBT	4.872	3.806	2.885	2.282	2.025	1.669	0.898

Table 4 Comparison of nondimensional first critical buckling load with different theories for different material distribution (L/h = 50, a = 0).

Theory	Ceramic	k = 0.3	k = 1	k = 3	k = 5	k = 10	Metal
CBT	4.906	3.812	2.905	2.305	2.047	1.688	0.904
FSDBT	4.902	3.809	2.902	2.302	2.045	1.685	0.903
PSDBT	4.901	3.808	2.902	2.301	2.044	1.685	0.903
ESDBT	4.901	3.811	2.902	2.301	2.044	1.685	0.903

Table 5 Comparison of nondimensional first critical buckling load with different theories for different material distribution (L/h = 100, a = 0).

Theory	Ceramic	k = 0.3	k = 1	k = 3	k = 5	k = 10	Metal
CBT	4.906	3.812	2.905	2.305	2.047	1.688	0.904
FSDBT	4.905	3.811	2.904	2.304	2.047	1.687	0.904
PSDBT	4.905	3.811	2.904	2.304	2.047	1.687	0.904
ESDBT	4.905	3.812	2.904	2.304	2.046	1.6867	0.904

It is worth investigating the significance of shear deformation not only on the critical buckling load but also on the resulting postbuckling response, which is considered to be the contribution of this study. The postbuckling response of simply supported FGM beams using Euler–Bernoulli's beam theory, Timoshenko's theory, and some higher-order shear deformation theories is presented.

Figures 3-4 shows the critical buckling load $\left(\overline{P}_{cr}\right)$ vs the nondimensional amplitude for different values of volume fraction exponent k (L/h = 5). It is seen that the nondimensional axial load increases monotonically as the nondimensional amplitude increases. The values of the nondimensional axial load calculated by using the some higher-order shear deformation theories are lower than those calculated by using the Timoshenko's theory, which is lower than those calculated by using the Euler–Bernoulli's beam theory.

Figures 5-6 shows the variation trend of nondimensional axial load with length-to-thickness ratios L/h for different values of material gradient index k. It is observed that with increasing the length-to-thickness ratios L/h from 5 to 20, the nondimensional axial load also increases steadily, whatever the material gradient index k is. It is also found that transverse shear deformation has some effect on the buckling load. As the length-to-thickness ratios increases, the difference between the values of higher-order shear deformation theories, Timoshenko's theory and Euler-Bernoulli's beam theory decreases.

As can be noted from the figures, the length-to-thickness ratio is a crucial parameter in the analysis of postbuckling of functionally graded beams. As Equation (6) shows the significance of this parameter in determining the critical buckling load, these figures show that it also has a significant effect on the postbuckling response. As the higher-order shear deformation theories show very close results in the course of the critical buckling load, they also yield similar postbuckling response. We also note that the first-order shear deformation theory always underestimates the amplitude of buckling compared with higher-order theories.
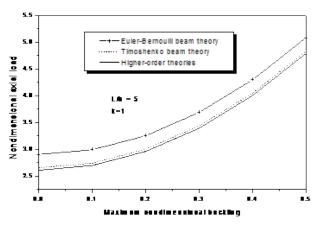
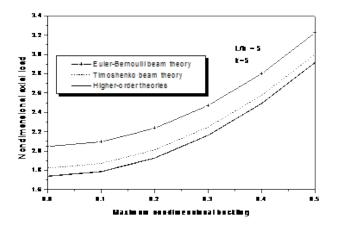**Fig. 3** Variation of the maximum buckling with the applied axial load for L/h = 5 and k = 1.

Fig. 4 Variation of the maximum buckling with the applied axial load for L/h = 5 and k = 5.
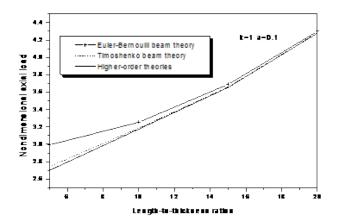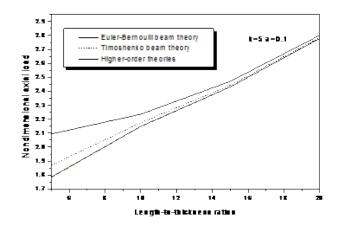

Fig. 5 Variation of the maximum buckling with the length-to-thickness ratio for a = 0.1 and k = 1.

Fig. 6 Variation of the maximum buckling with the length-to-thickness ratio for a =0.1 and k = 5.

4 Conclusion

In the present paper, equilibrium and stability equations for a simply supported rectangular functionally graded beam are obtained using the classical, first-order, and higher-order shear deformation theories, with the assumption of power law composition for the constituent materials. Closed form solutions for the critical buckling load and static postbuckling response of beams are presented. Numerical results show the significant effect of the shear deformation on the buckling and postbuckling responses of moderately thick beams or beams made of functionally graded materials. For instance, the critical buckling loads predicted by the classical beam theory and first-order shear deformation theory are underestimated. The effect of shear deformation on the static postbuckling response is also investigated. Using the first-order and some higher-order shear deformation theories, the amplitude of buckling is found to be much higher than its value predicted by the classical beam theory. It is also found out that higher-order shear deformation theories considered in this study have led to the same results for buckling and postbuckling responses. Based on the post-buckling response, one can conclude that the effect of the shear deformation has considerable effect on the critical buckling load of functionally graded beam, especially for a thick beam.

Acknowledgement

References

[1] Hetnarski, R. B., Eslami, M. R. "*Thermal stresses – advanced theory and applications*." Springer, 2009. DOI: 10.1007/978-1-4020-9247-3

[2] Noda, N. "Thermal stresses in functionally graded materials." *Journal of Thermal Stress*. 22(4-5), pp. 477-512. 1999. DOI: 10.1080/014957399280841

[3] Chakraborty, A., Gopalakrishnan, S., Reddy, J. N. "A new beam finite element for the analysis of functionally graded materials." *International Journal of Mechanical Sciences*. 45(3), pp. 519-539. 2003. DOI: 10.1016/s0020-7403(03)00058-4

[4] Zhao, F. Q., Wang, A. M., Liu, H. Z. "Thermal post-buckling analyses of functionally graded material rod." *Applied Mathematics and Mechanics*. 28(1), pp. 59-67. 2007. DOI: 10.1007/s10483-007-0107-z

[5] Li, S. R., Zhang, J. H., Zhao, Y. G. "Thermal post-buckling of functionally graded material Timoshenko beams." *Applied Mathematics and Mechanics*. 27(6), pp. 803-810. 2006. DOI: 10.1007/s10483-006-0611-y

[6] Rastgo, A., Shafie, H., Allahverdizadeh, A. "Instability of curved beams made of functionally graded material under thermal loading." *International Journal of Mechanics and Materials in Design*. 2(1-2), pp. 117-128. 2005. DOI: 10.1007/s10999-005-4446-3

[7] Ke, L. L., Yang, J., Kitipornchai, S. "Postbuckling analysis of edge cracked functionally graded Timoshenko beams under end-shortening." *Composite Structures*. 90(2), pp. 152-160. 2009. DOI: 10.1016/j.compstruct.2009.03.003

[8] Ke, L. L., Yang, J., Kitipornchai, S., Xiang, Y. "Flexural vibration and elastic buckling of a cracked Timoshenko beam made of functionally graded materials." *Mechanics of Advanced Materials and Structures*. 16(6), pp. 488-502. 2009. DOI: 10.1080/15376490902781175

[9] Reddy, J. N. "Analysis of functionally graded plates." *International Journal for Numerical Methods in Engineering*. 47, pp. 663-684. 2000. DOI: 10.1002/(sici)1097-0207(20000110/30)47:1/3<663::aid-nme787>3.0.co;2-8

[10] Vel, S. S., Batra, R. C. "Exact solution for thermoelastic deformations of functionally graded thick rectangular plates." *AIAA Journal*. 40, pp. 1021-1033. 2002. DOI: 10.2514/3.15212

[11] Vel, S. S., Batra, R. C. "Three-dimensional exact solution for the vibration of functionally graded rectangular plates." *Journal of Sound and Vibration*. 272, pp. 703-730. 2004. DOI: 10.1016/s0022-460x(03)00412-7

[12] Matsunaga, H. "Free vibration and stability of functionally graded plates according to a 2-D higher-order deformation theory." *Composite Structures*. 82(4), pp. 499-512. 2008. DOI: 10.1016/j.compstruct.2007.01.030

[13] Matsunaga, H. "Thermal buckling of functionally graded plates according to a 2D higher-order deformation theory." *Composite Structures*. 90(1), pp. 76-86. 2009. DOI: 10.1016/j.compstruct.2009.02.004

[14] Bouazza, M., Tounsi, A., Adda-Bedia, E. A., Megueni, A. "Thermal buckling behavior of functionally graded material." *Journal of Materials Science and Technology*. 18(3), pp. 155-170, 2010.

[15] Bouazza, M., Tounsi, A., Adda-Bedia, E. A., Megueni, A. "Stability analysis of functionally graded plates subject to thermal loads." In: *Shell-like Structure*. pp. 669-680. Springer, 2011. DOI: 10.1007/978-3-642-21855-2_44

[16] Bouazza, M., Tounsi, A., Adda-Bedia, E. A., Megueni, A. "Thermoelastic stability analysis of functionally graded plates: An analytical approach." *Computational Materials Science*. 49(4), pp. 865-870. 2010. DOI: 10.1016/j.commatsci.2010.06.038

[17] Bouazza, M., Ouinas, D., Abdelaziz, Y., Hamouine, A. "Buckling of thin plates under uniaxial and biaxial compression." *Journal of Materials Science and Engineering B*. 2(8), pp. 487-492. 2012.

[18] Brischetto, S., Leetsch, R., Carrera, E., Wallmersperger, T., Kröplin, B. "Thermomechanical bending of functionally graded plates." *Journal of Thermal Stress*. 31(3), pp. 286-308. 2008. DOI: 10.1080/01495730701876775

[19] Hosseini-Hashemi, Sh., Fadaee, M., Atashipour, S. R. "A new exact analytical approach for free vibration of Reissner–Mindlin functionally graded rectangular plates." *International Journal of Mechanical Sciences*. 53(1), pp. 11-22. 2011. DOI: 10.1016/j.ijmecsci.2010.10.002

[20] Reddy, J. N., Chin, C. D. "Thermo mechanical analysis of functionally graded cylinders and plates." *Journal of Thermal Stresses*. 21(6), pp. 593-626. 1998. DOI: 10.1080/01495739808956165

[21] Praveen, G. N., Reddy, J. N. "Nonlinear transient thermoelastic analysis of func- tionally graded ceramic-metal plates." *International Journal of Solids and Structures*. 35(33), pp. 4457-4476. 1998. DOI: 10.1016/s0020-7683(97)00253-9

[22] Soldatos, K. P., Timarci, T. "A unified formulation of laminated composite, shear deformable, five degrees of freedom cylindrical shell theories." *Composite Structures*. 25(1-4), pp. 165-171. 1993. DOI: 10.1016/0263-8223(93)90162-j

[23] Nayfeh, A. H., Mook, D. T. "*Nonlinear oscillations*." Wiley, New York. 1979.

[24] Hyer, M. W. "*Stress analysis of fiber-reinforced composite materials*." McGraw-Hill. 1998.

[25] Nayfeh, A. H., Emam, S. A. "Exact solution and stability of postbuckling configurations of beams." *Nonlinear Dynamics*. 54(4), pp. 395-408. 2008. DOI: 10.1007/s11071-008-9338-2

[26] Croce, L. D., Venini, P. "Finite elements for functionally graded Reissner–Mindlin plates." *Computer Methods in Applied Mechanics and Engineering*. 193(99-11), pp. 705-725. 2007. DOI: 10.1016/j.cma.2003.09.014

[27] Natarajan, S., Baiz, P. M., Bordas, S., Rabczuk, T., Kerfriden, P. "Natural frequencies of cracked functionally graded material plates by the extended finite element method." *Composite Structures*. 93(11), pp. 3082-3092. 2011. DOI: 10.1016/j.compstruct.2011.04.007

[28] Reddy, J. N. "*Mechanics of laminated composite plates*." CRC Press, Boca Raton. 1997.

[29] Timarci, T., Soldatos, K. P. "Comparative dynamic studies for symmetric cross-ply circular cylindrical shells on the basis of a unified shear deformable shell theory." *Journal of Sound and Vibration*. 187, pp. 609-624. 1995. DOI: 10.1006/jsvi.1995.0548

[30] Zhen, W., Wanji, C. "A higher-order theory and refined three-node triangular element for functionally graded plates." *European Journal of Mechanics A/ Solids*. 25(3), pp. 447-463. 2006. DOI: 10.1016/j.euromechsol.2005.09.009